Advances in Photogrammetry, Remote Sensing and Spatial Information Sciences:
2008 ISPRS Congress Book – Li, Chen & Baltsavias (eds)

CHAPTER 15

Object extraction and attribution from hyperspectral images

Freek van der Meer, Harald van der Werff, Mark van der Meijde, Frank van Ruitenbeek,
Chris Hecker & Steven de Jong

ABSTRACT: Spectral reflectance in the visible and near-infrared offers a rapid and inexpensive technique for determining the mineralogy of samples and obtaining information on chemical composition. Absorption-band parameters such as the position, depth, width and asymmetry of the feature have been used to quantitatively estimate composition of samples from hyperspectral field and laboratory reflectance data. The parameters have also been used to develop mapping methods for the analysis of hyperspectral image data. This has resulted in techniques providing surface mineralogical information (e.g. classification) using absorption-band depth and position; however, no attempt has been made to prepare images of the absorption-band parameters. In this chapter, a simple linear interpolation technique is proposed in order to derive absorption-band position, depth and asymmetry from hyperspectral image data. It is demonstrated that these absorption band maps provide basic information for surface compositional mapping. Next, we look at stratified image analysis approaches and data integration techniques. Lastly we use contextual information for image analysis. A full contextual image analysis approach is presented in the form of a template matching technique. Future challenges in the field of hyperspectral remote sensing are to fully explore spatial as well as spectral image characteristics for image classification, to couple image products to subsurface information, and to include temporal spectral variability as a means of characterizing geo-objects.

Keywords: Hyperspectral images, spectral matching, reflectance spectroscopy, contextual image analysis

15.1 INTRODUCTION: HYPERSPECTRAL REMOTE SENSING

Imaging spectrometers acquire imagery in many, narrow and contiguous spectral bands with the aim of collecting "image radiance or reflectance spectra" that can be compared with field or laboratory spectra of known materials. Imaging spectrometry has been widely used in geological mapping, specifically in so-called hydrothermal alteration systems. These are areas where the composition of host rocks is altered through the circulation of hot fluids giving rise to the formation of new mineral assemblages in a predefined order in (3-D) space. Surface mineralogical information can be derived from imaging spectrometer data by comparing imaged reflectance spectra of unknown composition to data from spectral libraries. This comparison is mostly done on a pixel-by-pixel basis. In general, a matching is done to express the similarity between the unknown pixel spectrum and known spectra from spectral libraries. As a result, in geology, information on surface mineralogy can be derived from imaging spectrometry data, which in turn can be incorporated into geologic models. Field and laboratory spectra have been used to relate absorption features to chemical composition of samples in both the areas of soil science and mineralogy, as well as in the area of vegetation science. For the analysis of hyperspectral image data, there are several techniques available to derive surface composition (e.g. surface mineralogy) from a combination of absorption-band position and depth. However, no such technique provides spatial information on the variation of absorption-band depth, position and shape despite the fact that these parameters are of vital use in quantitative surface compositional mapping.

Quantitative estimates of mineralogical composition and chemical analysis on the basis of spectroscopic data have been demonstrated by many authors. In this chapter, we evaluate pixel based methods of

hyperspectral data analysis to (1) derive surface compositional information, and (2) to derive absorption feature characteristics. We will highlight the intrinsic problems and solutions to these problems for these methods. Thereafter we will discuss contextual analysis techniques as an alternative approach. This chapter is written largely from a geological perspective on the present and future use of hyperspectral data. Although some remarks may be considered universal, it should be noted that not all presented results are equally applicable to other thematic fields. We also do not aim at providing a thorough and detailed review of the entire field, but merely try to sketch the development of hyperspectral remote sensing in geology providing a framework for future studies.

15.2 PIXEL-BASED METHODS FOR SPECTRAL MATCHING

15.2.1 *Introduction*

Most analytical techniques to handle hyperspectral data work on a pixel-by-pixel basis, either to (1) match known spectra with unknown pixel spectra to derive surface composition, or (2) to derive absorption band parameters that can yield input to empirical models.

15.2.2 *Spectral matching techniques*

Spectral matching techniques used for compositional mapping are various. Techniques to process hyperspectral imagery in order to obtain surface compositional information on a pixel-by-pixel basis for the entire image are reviewed by (Van der Meer et al. 2001). Techniques that specifically use absorption band position and depth include (1) the Relative Absorption Band-Depth (RBD) approach of Crowley et al. (1989), (2) the Spectral Feature Fitting (SFF) technique of Clark et al. (1990) and (3) the TRICORDER (Crowley & Swayze 1995) and TETRACORDER algorithms developed at the USGS spectral laboratory. These techniques work on so-called continuum removed reflectance spectra, thus acknowledging that the absorption in a spectrum has two components: a continuum and individual features. Crowley et al. (1989) developed a method of mineral mapping from imaging spectrometer using Relative Absorption Band-Depth Images (RBD) generated directly from radiance data. In essence, RBD images provide a local continuum correction removing any small channel to channel radiometric offsets, as well as variable atmospheric absorption and solar irradiance drop off for each pixel in the data set. To produce a RBD image, several data channels from both absorption band shoulders are summed and then divided by the sum of several channels from the absorption band minimum. The resulting absorption band-depth image gives the depth of an absorption feature relative to the local continuum, which can be used to identify pixels having stronger absorption bands indicating that these may represent a certain mineral.

Spectral feature fitting (embedded in the ENVI software) uses continuum removed pixel spectra, which are compared to continuum reference spectra of known mineralogy. A least squares fit is calculated band by band between each reference end-member and the unknown (continuum removed) pixel spectra. A "Scale" image is produced for each end-member selected for analysis by first subtracting the continuum-removed spectra from one, thus inverting them and making the continuum zero. A large scale-factor is equivalent to a deep spectral feature, while a small scaling factor indicates a weak spectral feature. A least squares fit is then calculated band by band between each reference end-member and the unknown spectrum. The total root mean square (RMS) error is used to form an RMS error image for each end-member. The ratio of the scale image and the RMS image provides a "Fit" image that is a measure of how well the unknown spectrum matches the reference spectrum on a pixel-by-pixel basis. The Tricorder and its successor Tetracorder use spectral matching algorithms carried out in a two step process. First, the local spectral slope (the "continuum") is estimated and removed both from reference and observed spectra. Next, the identification of materials from their spectra is constrained by (1) the goodness of fit of a spectral feature to a reference, (2) reflectance level, (3) continuum slope, and (4) presence or absence of key ancillary spectral features. The Tetracorder uses these reference continuum-removed-spectral features to compute a weighted fit between unknown spectra and known library spectra. By means of an expert system approach, surface compositional information is derived and results are validated. These mapping methods described all produce validated surface compositional information (mostly mineralogical maps), however do not provide information on the absorption band position, depth and asymmetry on a pixel by pixel basis although these parameters are used in the matching performed.

Since absorption band parameters are of importance to quantitative reflectance spectroscopy, attempts have been made to develop linear estimation methods to derive absorption band parameters from hyperspectral image data. Another spectral matching technique is the Cross correlogram spectral matching (CCSM; Van der Meer & Bakker 1997); an approach toward mineral mapping from imaging spectrometer data using the cross correlogram of pixel and reference spectra. A cross correlogram is constructed by calculating

the cross correlation at different match positions between a test spectrum (i.e. a pixel spectrum) and a reference spectrum (i.e. a laboratory mineral spectrum or a pixel spectrum known to represent a mineral of interest) by shifting the reference spectrum over subsequent channel positions. The statistical significance of the cross correlation coefficient can be assessed by a student's t-test and the skewness can be calculated as an estimator of the goodness-of-fit. The cross correlogram for a perfectly matching reference and test spectrum is a parabola around the central matching number (m = 0) with a peak correlation of 1. Deviations from this shape indicate a different surface mineralogy. Mineral mapping on a pixel-by-pixel basis is achieved by extracting three parameters from the cross correlograms and combining these into a statistical estimate of the goodness of fit of the two spectra compared: the correlation coefficient at match position zero, the moment of skewness (based on the correlation differences between match numbers of equal but reversed signs, e.g. m = 4 and m = -4), and the significance (based on a student t-test testing the validity of the correlation coefficient at m = 0). In order to evaluate the surface mineralogy maps, a root mean square error assessment procedure is proposed in Van der Meer & Bakker (1997), in which the error is calculated from the difference between the calculated pixel cross correlogram and the ideal cross correlogram calculated for the reference.

The most used mapping method in hyperspectral remote sensing is the spectral angle mapper. The spectral angle mapper calculates the spectral similarity between a test reflectance spectrum and a reference reflectance spectrum assuming that the data is correctly calibrated to apparent reflectance with dark current and path radiance removed. In this approach, the spectra are treated as vectors in a space with dimensionality equal to the number of bands, n.

The outcome of the spectra angle mapping for each pixel is an angular difference measured in radians. The main problem using the spectral angle mapper is the appropriate selection of the threshold to classify the derived rule images. Since the angle is neither a physical nor a statistical measure, there is no statistically/physically sound approach to do so. Some problems related to spectral matching techniques are illustrated in Figure 15.1. Here the correlation is calculated between a calcite laboratory spectrum (from the JPL 160 mineral library available in ENVI) and a dolomite spectrum and an iron rich dolomite spectrum. We calculate the correlation coefficient for parts of the spectrum starting with the first 800 (of a total of 826 channels of the Beckman spectrometer) channels and subsequently diminishing this number by steps of 50 channels such that at the end only the correlation between the 50 channels in the long

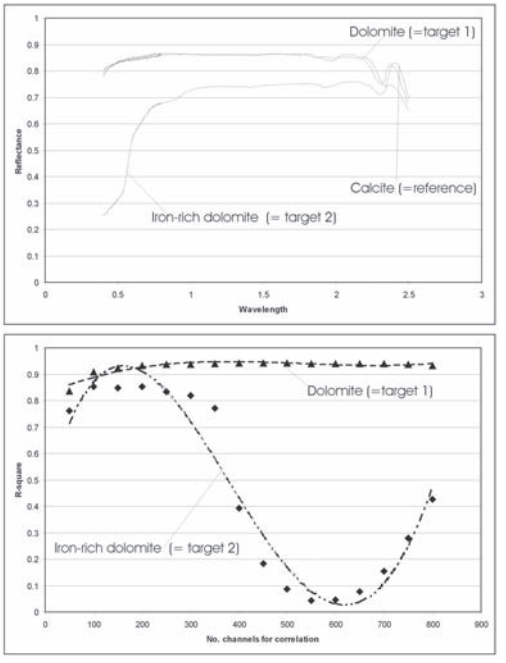

Figure 15.1. Correlation between calcite (reference) and dolomite (target 1) and iron-rich dolomite (target 2). See text for discussion.

wavelength portion of the SWIR are calculated. For the calcite versus dolomite spectrum, we notice that the correlation is high (0.93) and diminishing to 0.84 when using only the last 50 channels of the spectrometer. This can be explained by the fact that calcite and dolomite have an absorption band around 2.3 micron, which changes only from 2.35 to 2.3 micron for calcite versus dolomite.

Hence the significant difference in the two spectra is in this part of the spectrum. In fact, the graph shows that including other wavelengths only adversely influences the matching result. The same can be observed when looking at the correlation graph of the calcite versus the iron-rich dolomite spectrum. However, this graph shows various correlation maxima and minima because the shape of the graphs are similar in parts of the spectrum but differ, particularly in the visible part of the spectrum. Hence including irrelevant information severely damages the matching result. Another point arises in thresholding the correlation to perform a classification. How to objectively determine a threshold? This is a particular problem when using the SAM technique because the angles will vary non-linearly with the per cent spectrum mixed into a mixture.

15.2.3 *Absorption-band parameter estimation*

Alternative approaches fully exploit the spectral properties of absorption bands in hyperspectral data sets. The following absorption-band parameters calculated from continuum-removed spectra are often used: (1) the absorption-band position, (2) the absorption-band depth, and (3) the absorption-band asymmetry. The absorption band parameter definition as discussed above assumes nearly continuous (contiguous) spectral data, whereas imaging spectrometers acquire data in a large number of discrete spectral bands. The band centre wavelength position is usually employed for further calculations, thus providing spectral measurements on a discrete number of wavelength positions characterizing an absorption feature. To accommodate this, a simple linear method is proposed to calculate the absorption feature parameters from image data. Figure 15.2 graphically explains the procedure followed.

First, for the absorption feature of interest, the image bands are determined that would serve as the shoulders of the absorption feature. By definition, there is a short wavelength shoulder (shoulder 2, denoted by S_2 in Fig. 15.2) and a long wavelength shoulder (shoulder 1, denoted S_1 in Fig. 15.2). Next, the data are continuum removed using the mentioned shoulders as starting and ending points. Subsequently, two bands are selected as the absorption points which are used in the interpolation (points A_1 and A_2 in Fig. 15.2). From the interpolated wavelength, position (e.g. the wavelength of maximum absorption) can be found by interpolating between the shoulders and absorption points in the spectrum as

$$Absorption\_wavelength = -\left[\frac{C_1}{C_1+C_2} * (A_1 - A_2)\right] + A_1 \quad (1)$$

The associated absorption-band depth is derived as

$$Absorption\_depth = \left[\frac{S_1 - absorbtion\_wavelength}{S_1 - A_1}\right] * Depth_1 \quad (2)$$

An example of absorption bands calculated for a HyMAP data set acquired over a sedimentary sequence is given in Figure 15.3.

15.3 STRATIFIED ANALYSIS OF HYPER-SPECTRAL DATA

15.3.1 *Data stratification*

An alternative approach to thematic analysis of hyperspectral data is stratified analysis. The aim would be to stratify the data on known thematic data layers prior to analytical approaches being applied to the data. In many cases, field or thematic map data is available. This data can thus be used for data processing. One can imagine clustering a data set on mapping units

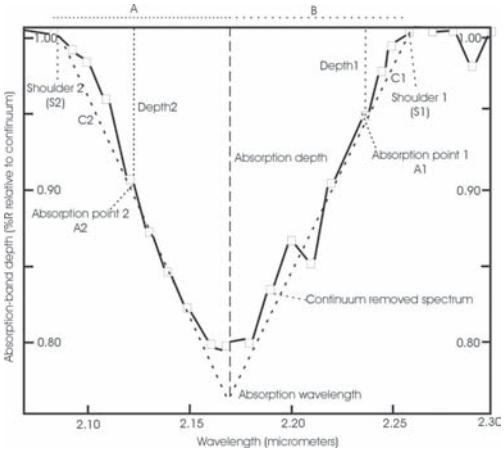

Figure 15.2. Definition of the parameters used in the linear interpolation of absorption feature characteristics.

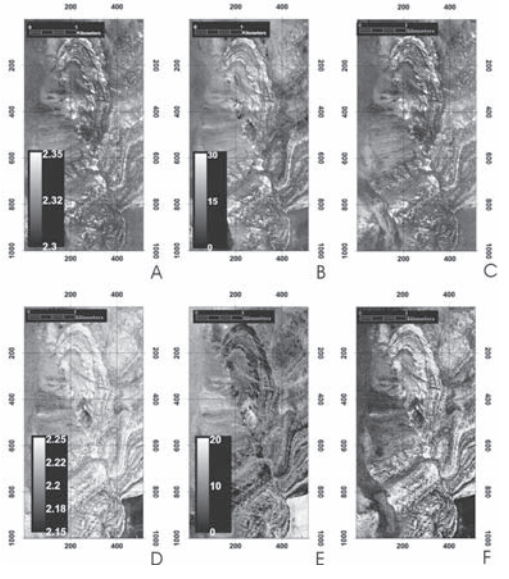

Figure 15.3. Absorption band parameters calculated from HyMAP data over a sedimentary terrain (A = carbonate absorption band wavelength position, B = depth of carbonate absorption band, C = asymmetry of the carbonate absorption band, D = absorption band wavelength for OH features in SWIR, E = depth of OH feature, F = asymmetry of the OH feature).

and starting the analysis within these natural boundaries. Furthermore, various data products from hyperspectral data sets can be integrated using statistical techniques. As an example we look at Probe-1 (also known as HyMAP) from an area in California (Santa Barbara) known for the presence of oil/gas seeps. These seeps can be detected in hyperspectral imagery either through (1) anomalous spectral behaviour of the vegetation, or (2) through mineral alteration in the soil. When evaluating the imaged area in terms of vegetation properties in relation to the lithology, we can clearly see the necessity for performing a stratified analysis. We calculated (1) the NDVI, (2) the carter stress ratio of band 695 nm over band 420 nm, (3) the carter stress ratio of band 695 nm over band 760 nm, and (4) the red edge inflection point. The so-called Carter ratio's (Carter 1994) are band ratios that are sensitive to vegetation stress. We computed these two ratios, 695/420 and 695/760, on a vegetation masked image (that is on pixels that have a NDVI value of greater than 0.5). Similarly we calculate the red edge inflexion point. In Table 15.1 we summarize the results of these calculations for number of key lithologies in the imaged area. The Monterey formation is the oil-producing unit.

15.3.2 *Example from Santa Barbara (Ca.)*

Hence, we first separated the data into a vegetation and a soil component by simply masking the data using the NDVI. Next, we stratified the data on the known geological units since these not only affect the soil type and hence the vegetation type but there is also a strong link between seepage and lithology. The main oil reservoir rock at some areas outcrops thus allowing seepage of oil to the surface. Seeps are also more likely to appear in gas form when sitting close to the host reservoir rock. The main derivative of interest for gas seepage in the vegetated areas is the red edge position, which can be regarded as an indicator of health status of the vegetation. In the soil component, we singled out various mineral maps (using spectral matching techniques described earlier) in particular iron oxides and enrichment in kaolinite and carbonate, which are indicative for seepage. These data layers for each unit were integrated using statistical approaches. The resulting spatial patterns were integrated with known oil and gas seeps using a spatial data integration approach (SDI). The basic proposition, the mathematical hypotheses that we want to test in this study—the presence or absence of an undiscovered oil/gas reservoir—is formulated. The probabilistic theory embedded in the favourability function allows this proposition to be addressed.

Table 15.1. Typical values of vegetation parameters for selected lithologies in the Santa Barbara imaged area.

	Vegetation		Stress ratio	
Lithology	NDVI	Red edge	695/760	695/420
Repetto	0.2–0.3	725	<0.2	0.65–1.25
Monterey	0.6–0.8	712	0.3–0.5	0.5–0.75
Sisquoc	0.5–0.8	715	0.2–0.3	0.99–1.2
Sespe	0.3–0.5	721	0.1–0.3	1.25–1.5

The favourability function method requires the two assumptions that: (i) past occurrences of a given type (i.e. a clearly identified type of process) can be characterized by sets of layers of supporting spatial data, and that (ii) new discoveries of the same type will occur in the future under similar circumstances. That is, the present should be able to predict the future. Consider a probability at any A, prob{Fp}, for the proposition Fp. This prior probability, a pixel p will contain a future reservoir, is obtained by

$$\text{Prob}\{\text{Fp}\} = \text{size of F/size of A} \tag{3}$$

where F denotes the unknown areas that will be reservoirs within A and "size of B" represents the size of the surface area covered by any sub-area B in A. Prob$\{F_p\}$ has the same value for all p. The purpose of the modelling is to see how the probability at p will be changed as we observe the m pixel values at p. At pixel p, the pixel value $v_l(p)$ of the l_{th} layer is c_l, which is one of the n_l classes (map units), {1, 2, … , n_l}. Consider a set of all pixels whose value in the 1st layer is c_l. The set is the thematic class in the 1st layer whose pixel value is c_l. The set is denoted by A_lc_l and it is one of the non overlapping nl sub-areas $\{A_{11}, A_{12}, \dots, A_1n_l\}$ in the 1st layer. Assume that the occurrences at each pixel p can be expressed as the joint conditional probability

$$Prob\{F_b / C_c, C_2 .... C_m\} \tag{4}$$

that p will be a future undiscovered oil/gas reservoir assuming that the p contains the m values, (c_1,c_2…cm). When eq.4 is approximately similar to Prob$\{F_p\}$ we can state that the pixel values at the p, (c_1,c_2…c_m) do not add any useful information as to whether the pixel is a undiscovered reservoir.

However, if

$$Prob\{F_b / C_c, C_2 .... C_m\} >> Prob\{F_b\} \tag{5}$$

or

$$Prob\{F_b / C_c, C_2 .... C_m\} << Prob\{F_b\} \tag{6}$$

then the pixel values, (c_1,c_2…c_m) provide very significant information and they are highly correlated either positively or negatively with occurrences. We assume that c_1, will contain an undiscovered oil/gas reservoir and we assume that the c_1,…c_m are conditionally independent given the condition F_p, (p will contain an undiscovered oil/gas reservoir). Hence, under the above conditional independence assumption, the joint conditional probability becomes

$$\frac{Prob\{C_1\}\ldots Prob\{C_m\}}{\Pr ob\{C_1,\ldots C_m\}} Prob\{F_b\} \frac{\Pr ob\{F_b/C_1\}}{\Pr ob\{F_b\}}\cdots\frac{\Pr ob\{F_b/C_m\}}{\Pr ob\{F_b\}} \quad (7)$$

Under the conditional independence assumption, this joint conditional probability can be expressed in terms of three components. The first component, the ratio of prob{c_1}… prob{c_m} and prob{c_1,…,c_m} consists of the probabilities related to the input spatial data. The second component, the prior probability Prob{F_p}, is the probability that a pixel p will be an undiscovered reservoir prior to having any evidence.

In Figure 15.4, we provide an interpretation of the patterns observed. Particularly the predicted probability map for the mineral alteration provides spectacular results. The image clearly shows an elliptical pattern of high probability values around the actual seep location forming what appears to be a halo. In the centre of the halo, low values give the appearance of a clogged area similar to the resulting patterns described in edge-leakage. The vegetation stress analysis in this area did reveal less information, which is due to the fact that few pure vegetation pixels are found and that large parts over the anomalous area are relatively devoid of vegetation.

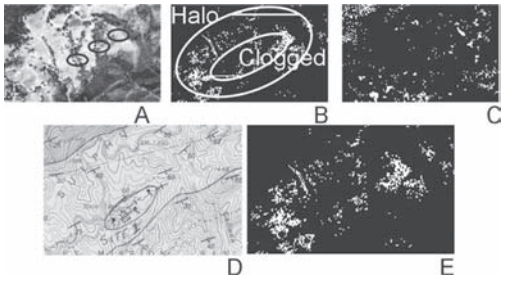

Figure 15.4. Results and interpretation. False colour image of probe bands 16, 9, 4 in RGB with seeps (A), SDI probability minerals with interpretation of the anomaly (B) SDI probability vegetation (C), geological map (D) and SDI probability minerals with annotation. All probability maps display P > 0.8. (see colour plate page 500)

15.4 CONTEXTUAL ANALYSIS OF HYPER-SPECTRAL IMAGERY

15.1.6 *Stratified approaches*

Stratified approaches are one step in the direction of using prior and thematic information in the analysis of hyperspectral data sets. A next step would be to include spatial and contextual information. Pixel-based methods described earlier have in common that they yield surface compositional information (e.g. in geological applications this is often surface mineralogy) that has to be further translated into a geological model (which involves understanding the spatial context of surface mineralogy). Furthermore, these models bypass the common notion in geology that spatial (contextual) information provides valuable information to infer the transitional nature of geological context. In other words, field geologists working in, for example, hydrothermal alteration systems use mineral paragenesis and the mineral assemblage in their mapping. When identifying a certain suite of minerals at a location, not only do they know in which part of the alteration system they are spatially, but also from this information they can infer which mineralogic transition they are about to discover when progressing through the terrain. Hence, not only do they use information on the surface mineralogy, but also they use neighbourhood information to unravel the geologic history and alteration system of an area.

15.1.7 *True contextual image analysis*

To combine both spectral as well as spatial information in the analysis of hyperspectral imagery, we have developed a spatial spectral algorithm; the template matching algorithm (Van der Werff et al. 2007). A template consists of a one- or two-dimensional array that is filled on both sides of a central pixel with spectra (or spectral derivatives such as ratios, etc.) that characterize certain cover types of interest. The template is matched with an image by moving the kernel or a filter over the image and calculating parameters at each pixel. At each pixel, the template is also rotated and the following parameters are calculated: the best template fit, the worst template fit, the mean template fit, the variance in template fit, the mean variance in fit of individual pixels, the variance in variance in fit of individual pixels, and the optimal scan angle, which is the angle belonging to the best template fit.

The Template-fit is the total value for N number of pixels; a mean fit is derived as:

$$\overline{F}_p = \frac{\Sigma_{p=0}^{N} F_{(p)}}{N} \quad (8)$$

The variance in pixel fit, the Template fit Variance layer, is calculated for the template as:

$$V_p = \frac{\Sigma_{p=0}^{N}\left(F_{(p)} - \overline{F}_p\right)^2}{N} \quad (9)$$

When the template is rotated, for every orientation (every scan angle) of the template the extreme values are stored as "Best Template Fit" and "Worst Template Fit". The optimal scan angle is set to the scan angle (best orientation) that gave "Best Fit Template"; otherwise variance in template fit cannot be determined. The "Mean Template Fit" is calculated using:

$$\overline{F}_T = \frac{\Sigma_{a=0}^{A}\overline{F}_{p(a)}}{A} \quad (10)$$

where A is the number of scan angles. The variance in template fit is calculated by:

$$V_T = \frac{\Sigma_{a=0}^{A}\left(\overline{F}_{p(a)} - \overline{FT}\right)^2}{A} \quad (11)$$

Figure 15.5 shows the principle of template matching whereas Figure 15.6 shows some results of template matching on synthetic image lines showing the improved capabilities for detecting crisp and fuzzy boundaries.

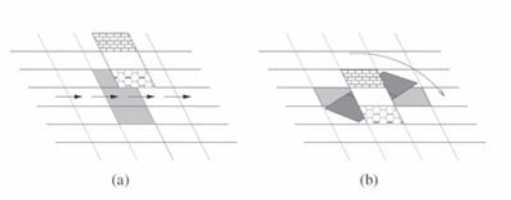

Figure 15.5. Principle of template matching. A micro image is defined on the basis of spectral characteristics of two classes with crisp or fuzzy boundaries (A) and swept over the hyperspectral image to calculate a spatial correlation (B).

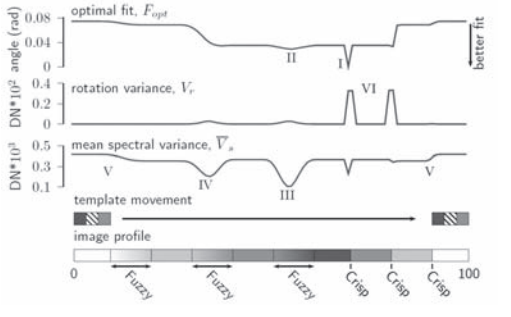

Figure 15.6. Results of template matching on synthetic image line showing the improved capabilities for detecting crisp and fuzzy boundaries.

15.5 CHALLENGES

In this chapter we have sketched a development in the field of hyperspectral remote sensing for geological applications from pixel based to context based approaches. Early work relied on statistical matching of pixel spectra to library spectra to come to image products useful for geology. In the early 2000s, the work started to include stratified approaches, data integration approaches and geo-inversion. More recently researchers looked at segmentation and contextual approaches to couple spectral as well as spatial information in hyperspectral data. Most image processing techniques that are available to analyse hyperspectral data by-pass three important aspects of remote sensing: (1) neighbourhood information is not incorporated and hence the common knowledge formulated in geo-statistics that nearby control points are more likely to contain information more similar than far apart control points, (2) surface information is not coupled to shallow subsurface information, although many problems are in need of a 3-dimensional approach of study, and (3) the change over time of the spectral signature of certain Earth surface materials that contains information on the type (and use) of the material at hand that may allow a better classification and or discrimination (from other) of materials is not used in sub-pixel classification. The challenge ahead lies in a full incorporation of the 3-D space and the 4-D temporal space to characterize image elements.

15.6 CONCLUSIONS

Reflectance spectroscopy has been used to derive estimates of soil/rock geochemistry and foliar biochemistry using, to date, mostly field and laboratory spectroscopic techniques. These techniques most often make use of absorption feature characteristics (e.g. absorption band wavelength position, depth and asymmetry), which are combined with geochemical analysis in a multi-linear regression to find empirical relationships with the chemistry of a sample. Absorption features have also been used as input to spectral feature fitting techniques that allow mapping surface composition (mainly mineralogy) from hyperspectral image data. However, by this process, the absorption feature analysis is confined to input data in a feature fitting. A simple linear interpolation method is introduced to estimate absorption-band parameters from hyperspectral image data. By applying

this hyperspectral data it has been demonstrated that absorption feature maps correspond favourably with the main alteration phases characterizing the systems studied. Thus, the derived feature maps allow enhancement of the analysis of airborne hyperspectral image data for surface compositional mapping. The next step is to expand in the direction of stratified analysis of hyperspectral data. This allows the incorporation of prior information into the analysis of hyperspectral data sets. The last example we present is using spatial information in full contextual analysis of hyperspectral data sets. In this case study, we deploy Markov chain analysis to include the repetitive patterns in a sedimentary sequence for the study of hyperspectral data sets. Overall with this chapter, we wish to advocate including both prior knowledge as well as spatial contextual information as an essential step forward in the science of hyperspectral remote sensing. An overview of contextual image analysis approaches is found in De Jong & Van der Meer (2004).

REFERENCES

Carter, C.A. 1994. Ratios of leaf reflectances in narrow wavebands as indicators of plant stress. *International Journal of Remote Sensing* 15: 697–703.

Clark, R.N., Gallagher, A.J. & Swayze, G.A. 1990. Material absorption band depth mapping of imaging spectrometer data using the complete band shape least-squares algorithm simultaneously fit to multiple spectral features from multiple materials. *Proceedings of the Third Airborne Visible/Infrared Imaging Spectrometer (AVIRIS) Workshop*: 176–186. Los Angeles: JPL Publication 90–54.

Crowley, J.K., Brickey, D.W. & Rowan, L.C. 1989. Airborne imaging spectrometer data of the Ruby mountains, Montana: mineral discrimination using relative absorption band-depth images. *Remote Sensing of Environment* 29: 121–134.

Crowley, J.K. & Swayze, G.A. 1995. Mapping minerals, amorphous materials, environmental materials, vegetation, water, ice, and other materials: The USGS Tricorder Algorithm. *Summaries of the Fifth Annual JPL Airborne Earth Science Workshop*: 39–40. Los Angeles: JPL Publication 95–1.

De Jong, S. & Van der Meer, F. 2004. *Remote sensing image analysis: including the spatial domain.* Dordrecht: Springer-Kluwer Academic Publishers.

Van der Meer, F. & Bakker, W. 1997. Cross Correlogram Spectral Matching (CCSM): application to surface mineralogical mapping using AVIRIS data from Cuprite, Nevada. *Remote Sensing of Environment* 61: 371–382.

Van der Meer, F., De Jong, S. & Bakker, W. 2001. Imaging spectrometry: Basic analytical techniques. In F. van der Meer & S. de Jong (eds), *Imaging Spectrometry: Basic Principles and Prospective Applications*: 17–61. Dordrecht: Kluwer Academic Publishers.

Van der Werff, H., Van Ruitenbeek, F., Van der Meijde, M., Van der Meer, F., De Jong, S. & Kalubandara, S. 2007. Rotation-variant template matching for supervised hyperspectral boundary detection. *IEEE Geoscience and Remote Sensing Letters* 4(1): 70–74.

Yang, H., van der Meer, F., Bakker, W. & Tan, Z.J. 1999. A back-propagation neural network for mineralogical mapping from AVIRIS data. *International Journal of Remote Sensing* 20: 97–110.